nonuniform filterbank are chosen as $m = 189$ and $c = 1$, whereas the desired amplitude responses of the filters are defined as $A_{d_i}(\omega) = \begin{cases} 1, & \omega \in B_i^p \\ 0, & \omega \in B_i^s \end{cases}$ for $i = 0, 1, 2$.

Based on the above specifications and the parameters chosen, the nonuniform transmultiplexer design problem can be readily formulated as a semi-infinite programming problem discussed in Section III. It can then be solved via the dual parameterization method. For the details of the theory and the algorithm of solving semi-infinite programming problem via the dual parameterization method, see [4] and [5].

By applying the dual parameterization method, a solution is obtained for a given set of transmitter coefficients. After three iterations between the filters designed for the transmitter and the receiver, the filter coefficients in both the transmitter and receiver converge. The magnitude response of the receiver filters and the transmitter filters are plotted as solid lines in, respectively, Figs. 2 and 3. The amplitude and aliasing distortions are shown in Fig. 4. To implement the existing method, we employ 15 674 grid points for the discretization method via the convex quadratic programming solver in MATLAB. The magnitude response of the receiver filters and the transmitter filters are plotted as dotted lines in, respectively, Figs. 2 and 3. The corresponding amplitude and aliasing distortions are shown in Fig. 4. We compared the results and found that the continuous constraints between some discretization points are not satisfied. Our algorithm overwhelmingly produces better results on suppressing the amplitude and aliasing distortions. According to the computer simulation, our algorithm can obtain about a 250-dB improvement for both the real and imaginary parts of both the amplitude and aliasing distortions. The amplitude distortion and the aliasing distortion are dramatically reduced from the order of 10^{-3} to 10^{-15} and 10^{-3} to 10^{-18}, respectively.

To further demonstrate the effectiveness of our proposed algorithm, three random signals with zero mean and unit variance are taken as the input signals for the nonuniform transmultiplexer. The mean square errors of these three channels are 1.3063×10^{-29}, 2.7917×10^{-29}, and 8.8908×10^{-30}, respectively. They are negligible for most engineering applications, and the nonuniform transmultiplexer can be regarded as a perfect reconstruction system.

V. Conclusion

The main contribution of this paper is the formulation of a nonuniform FIR transmultiplexer design problem as a *semi-infinite* programming problem. The method is based on the dual parameterization method. One of the advantages of this method is that it is guaranteed to achieve the global minimum while satisfying the passband and stopband specifications as well as the amplitude and aliasing requirements if the solution exists. It also avoids the problems occurred in the existing *semi-definite* programming approaches [6].

References

[1] R. D. Koilpillai, T. Q. Nguyen, and P. P. Vaidyanathan, "Some results in the theory of crosstalk-free transmultiplexers," *IEEE Trans. Signal Process.*, vol. 39, no. 10, pp. 2174–2183, Oct. 1991.

[2] T. Liu and T. Chen, "Design of multichannel nonuniform transmultiplexers using general building blocks," *IEEE Trans. Signal Process.*, vol. 49, no. 1, pp. 91–99, Jan. 2001.

[3] P. Q. Hoang and P. P. Vaidyanathan, "Non-uniform multirate filter banks: theory and design," in *Proc. IEEE Int. Symp. Circuits Syst.*, vol. 1, 1989, pp. 371–374.

[4] Y. Liu, K. L. Teo, and S. Ito, "Global optimization in quadratic semi-infinite programming," *Comput.*, vol. 15, pp. 119–132, 2001.

[5] C. H. Tseng, K. L. Teo, Z. Zang, and A. Cantoni, "A dual approach to continuous-time envelope-constrained filter design via orthonormal filters," *IEEE Trans. Circuits Syst. I: Funda. Theory Appl.*, vol. 46, no. 9, pp. 1042–1054, Sep. 1999.

[6] W. S. Lu, "A unified approach for the design of 2-D digital filters via semidefinite programming," *IEEE Trans. Circuits Syst. I: Funda. Theory Appl.*, vol. 49, no. 6, pp. 814–826, Jun. 2002.

The Reconstruction of Discontinuous Piecewise Polynomial Signals

Craig S. MacInnes, *Member, IEEE*

***Abstract*—The Gibbs phenomenon was recognized as early as 1898 by Michelson and Stratton. Gibbs oscillations occur during the reconstruction of discontinuous functions from a truncated periodic series expansion, such as a truncated Fourier series expansion or a truncated discrete Fourier transform expansion. Recent theoretical results have shown that Gibbs oscillations can be removed from the truncated Fourier series representation of a function that has discontinuities. This is accomplished by a change of basis to the set of orthogonal polynomials called the Gegenbauer polynomials. In this correspondence, a straightforward numerical procedure for the denoising of piecewise polynomial signals is developed. Examples using truncated Fourier series and discrete Fourier transform (DFT) series demonstrate the effectiveness of the numerical procedure.**

***Index Terms*—Denoising, discrete Fourier transform, Fourier series, Gegenbauer polynomials, Gibbs oscillations, signal reconstruction.**

I. Introduction

Classically, Gibbs oscillations occur when a discontinuous function is reconstructed from a truncated Fourier series expansion. Gibbs oscillations can also occur when sets of basis functions other than sinusoids are used, such as Fourier-Bessel series [1], wavelets [2], spherical harmonics [3], and Chebyshev polynomials [4]. Recent theoretical results have shown that the Gibbs oscillations can be removed using only the reconstructed function containing the Gibbs oscillations. This reconstruction can be carried out by a change of basis from the functions in the original truncated Fourier expansion to the set of Gegenbauer polynomials [5]. Furthermore, the reconstruction from the truncated Fourier series can be calculated with exponential accuracy, even at the points of discontinuity. It has been shown that there exists a set of functions $\{\omega_n(t)\}$ such that given an $\epsilon > 0$, there exists a $\gamma > 0$ and a value for M such that

$$\max_{-1 \le x \le 1} |f(t) - \omega_M(t)| \le e^{-\gamma M} \le \epsilon. \tag{1}$$

The significance of this is that function values that are close to a discontinuity can be recovered accurately as well as function values that are located away from the discontinuity. The function $\omega_M(t)$ in (1) represents a weighted sum of the first M Gegenbauer polynomials:

$$\omega_M(t) = \sum_{n=0}^{M-1} \mu_n C_n^{\alpha}(t).$$

Manuscript received March 10, 2004; revised July 27, 2004. The associate editor coordinating the review of this manuscript and approving it for publication was Dr. Jonathon A. Manton.

The author is with the Folium Algorithm Solutions Inc., Cranston, RI 02920 USA (e-mail: macinnescs@ieee.org).

Digital Object Identifier 10.1109/TSP.2005.849217

The signals considered in this paper are piecewise polynomial signals, i.e., signals that have contiguous sections, which are weighted sums of the monomials $1, t, t^2, \ldots$, which are simply the analytic monomial functions $1, z, z^2, \ldots$ defined on the entire complex plane and, here, restricted to the real line. The requirement of the analyticity of each signal segment in the original theorem [4] is therefore satisfied. In this corespondence, a Fourier series expansion truncated to N terms will be denoted by the function $\mathcal{FS}_N(t)$ and a discrete Fourier transform (DFT) series expansion truncated to N terms is denoted as $\mathcal{DS}_N(t)$. In Section II, the problem is described using an analysis of the so-called ramp function $f(t) = t$. In Section III, the Gegenbauer polynomials are defined, and in Section IV, a numerical procedure implementing the theoretical results is developed. In Section V, an application involving the denoising of a discontinuous signal is presented. Conclusions are presented in Section VI.

II. Analysis of the Ramp Function

Let a real-valued signal $x(u)$ be defined on the interval $u \in [a, b]$. The change of coordinates $t = -1 + 2(u - a)/(b - a)$ transforms the problem to one where $x(t)$ is defined on the interval $t \in [-1, 1]$, and therefore, all functions can be considered to be defined on the interval $[-1, 1]$ without loss of generality. The truncated Fourier series representation, $\mathcal{FS}_N(t)$ for $x(t)$ on $[-1, 1]$ can be written as a finite weighted sum of sinusoids:

$$f(t) \approx \mathcal{FS}_N(t) \equiv \frac{a_0}{2} + \sum_{k=1}^{N-1} \left(a_k \cos(\pi k t) + b_k \sin(\pi k t)\right).$$

It is a well-known fact [6] that at a point of discontinuity t_0, the truncated Fourier series $\mathcal{FS}_N(t)$ does not converge in the sup-norm to $f(t)$ for any value of N. In other words, given a value of N, there exists a constant κ such that $\sup_{[-1,1]} |f(t) - \mathcal{FS}_N(t)| > \kappa$ for any N. The nonvanishing oscillatory behavior of $\mathcal{FS}_N(t)$ near the point of discontinuity t_0 is commonly referred to as the Gibbs phenomenon.

At a point of discontinuity t_0 with $f(t_0-) > f(t_0+)$, the maximum value of $f(t)$ in an interval sufficiently small to the left of t_0 for large N is approximately [7]

$$\begin{aligned}\max(f(t_0-)) &\approx f(t_0-) + \frac{f(t_0-) - f(t_0+)}{\pi} \\ &\quad \times \int_{\pi}^{\infty} \frac{\sin(\alpha)}{\alpha} d\alpha \\ &\approx f(t_0-) + (f(t_0-) - f(t_0+)) \\ &\quad \times (0.089\,489\,9).\end{aligned}$$

For the ramp function $f(t) = t$, the magnitude of the discontinuity at $t = 1$ is 2, and therefore, the amount of overshoot at a point to the left of $t_0 = 1$ is approximately 17.9% for large N. As N increases, the peak of the largest oscillation moves closer to 1 from the left, with a similar movement of the minimum value of the corresponding oscillation toward -1 from the right.

In order to examine the Gibbs oscillations more closely, start with the Fourier series for $r(t) = t$:

$$\begin{aligned}t = \frac{2}{\pi}\sin(\pi t) - \frac{2}{2\pi}\sin(2\pi t) \\ + \frac{2}{3\pi}\sin(3\pi t) - \cdots + (-1)^{n-1}\frac{2}{n\pi}\sin(n\pi t) + \cdots. \quad (2)\end{aligned}$$

Plots of truncated series reconstructions of $r(t)$ for Fourier and DFT series are given in Fig. 1. In the top plot, $\mathcal{FS}_4(t)$ and $\mathcal{FS}_8(t)$ are given. Since the sinusoids in the Fourier series are of the form $\sin(2\pi(n/2)t)$, the sequence of terms are in 0.5 Hz increments, and therefore, the two reconstructions involve truncations to 2 and 4 Hz, respectively.

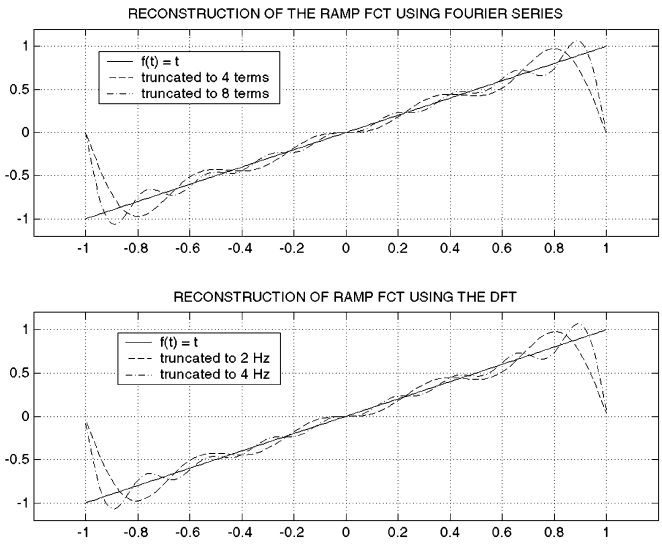

Fig. 1. Gibbs oscillations for reconstruction of $f(t) = t$.

The function $r(t)$ on $[-1, 1]$ was then sampled at a rate of $f_s = 100$ Hz. A 200-point DFT was then calculated, giving $\Delta f = 0.5$ Hz and a Nyquist frequency of 50 Hz. Pairs of DFT coefficients $\{\eta_n, \bar{\eta}_{-n}\}$ corresponding to both positive and negative frequencies were retained, and the DFTs did not involve windowing. The truncation to 2 Hz involved retaining nine DFT coefficients, and the truncation to 4 Hz retained 17 DFT coefficients. Graphs of the reconstructed signals are given in the bottom plot of Fig. 1. From a signal processing viewpoint, the nine-term truncated DFT corresponds to the application of a frequency domain rectangular bandpass filter with a 2-Hz cut-off frequency and the 17-term truncation has a 4-Hz cut-off frequency, with no windowing used prior to calculation of the DFT. Since the Nyquist frequency was 50 Hz, and the ramp function is not bandlimited, the truncated DFT series reconstructions includes aliasing effects. It can be seen from the plots that there are also oscillations away from the discontinuity at ± 1. This is due to the slow $(1/n)$ rate of decrease in the magnitude of the Fourier series coefficients, as given in (2). With a view toward engineering applications, N-term DFT series approximations of functions, which are denoted by $\mathcal{DS}_N(t)$, will be considered as well as N-term Fourier series approximations $\mathcal{FS}_N(t)$ in the following discussions. In order to remove the Gibbs oscillations, expansions of either $\mathcal{FS}_N(t)$ or $\mathcal{DS}_N(t)$ in terms of the set of real-valued orthogonal polynomials called the Gegenbauer polynomials must be obtained. In Section III, some of the properties of the Gegenbauer polynomials are discussed.

III. Properties of the Gegenbauer Polynomials

The Gegenbauer, or ultraspherical polynomials, $C_n^{\alpha}(t)$ are a series of polynomials that are orthogonal on the interval $[-1, 1]$, with respect to the weight function $w(t) = (1 - t^2)^{\alpha - 1/2}$, where $\alpha > -1/2$. They are defined by

$$\int_{-1}^{1} (1 - t^2)^{\alpha - 1/2} C_k^{\alpha}(t) C_n^{\alpha}(t) dt = \delta_{n,k} \rho_n^{\alpha}$$

where $\delta_{n,k}$ is the Kronecker delta function and where the normalization constants are defined by

$$\rho_n^{\alpha} = \|C_n^{\alpha}(t)\|_2^2 = \pi^{1/2} \frac{\Gamma(n + 2\alpha)\Gamma\left(\alpha + \frac{1}{2}\right)}{n!\Gamma(2\alpha)\Gamma(\alpha)(n + \alpha)} \quad (3)$$

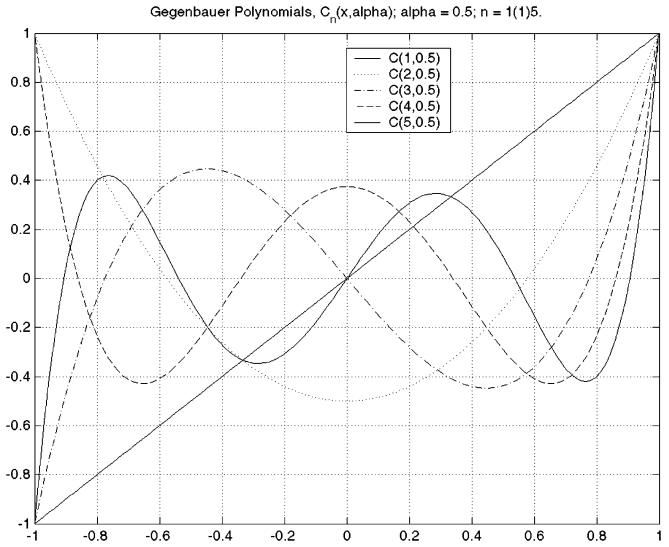

Fig. 2. First five unnormalized Gegenbauer polynomials.

where $\Gamma(t)$ is the Gamma function [8]. The first two Gegenbauer polynomials are $C_0^\alpha(t) = 1$ and $C_1^\alpha(t) = 2\alpha t$. The remaining polynomials can be defined recursively by

$$C_{n+1}^\alpha(t) = \frac{2(n+\alpha)tC_n^\alpha(t) - (n+2\alpha-1)C_{n-1}^\alpha(t)}{n+1}$$
$$n = 1, 2, \ldots$$

so that $C_2^\alpha(t) = 2\alpha(1+\alpha)t^2 - \alpha$, etc. The unnormalized Gegenbauer polynomials $C_n^\alpha(t)$ for $n = 1$ to 5 for $\alpha = 0.5$ are plotted in Fig. 2. Here, $C(1, 0.5)$ denotes $C_1^{0.5}(t)$. In general, $C_n^\alpha(-1) = -1$ for odd n and 1 for even n, and $C_n^\alpha(1) = 1$ for all n. The normalized Gegenbauer polyonmials are defined using (3) by $\widetilde{C}_n^\alpha(t) \equiv C_n^\alpha(t)/\sqrt{\rho_n^\alpha}$.

IV. Analysis and Reconstruction Using the DFT

The rearranged DFT matrix $\mathcal{D}$ for an N-point DFT that will be used in the analysis and reconstruction algorithms developed here is obtained by ordering the columns of the conventional DFT matrix from the most negative to the most positive frequency and then scaling by $1/\sqrt{N}$ so that $\mathcal{D}$ is unitary, and therefore, Parseval's relation holds without the need for a scaling factor, i.e., $\|\mathcal{D}(f)\|_2 = \|f\|_2$. This definition of the DFT and a corresponding scaling for Fourier series transforms make them unitary transforms, i.e., transforms that preserve the 2-norm of a function.

Let a function $f(t)$ defined on $[-1, 1]$ be sampled at N points at the sampling rate $f_s = 100$ Hz, followed by an N-point DFT $\mathcal{D}_N f$. The $(2M+1)$-vector $c = [c_{-M} \cdots c_M]^T$ representing the DFT coefficients corresponding to the $2M+1$ smallest magnitude frequencies is then selected. Here, the term with index zero corresponds to the DC component. The elements of c are then the DFT coefficients of a truncated DFT series. We define the matrix F_M as the $N \times 2M+1$ submatrix of the $N \times N$ DFT matrix $\mathcal{D}$. The columns of F_M are orthonormal, due to the scaling operation discussed above.

Let g_0 be an N-vector derived from a function $g(t)$, which has been sampled at $N > 2M+1$ equally spaced points $t_1, \ldots, t_N$. The $(2M+1)$-term truncated DFT series coefficients expressed in vector form can then be found simply by calculating $c = F_M^T g_0$. The reconstruction of g_0 from its truncated discrete Fourier series is then accomplished by calculating the matrix-vector product $\tilde{g}_0 = F_M c$. The two operations involving the determination of the DFT coefficients and the reconstruction can be combined to yield

$$\tilde{g}_0 = F_M c = F_M F_M^T g_0. \tag{4}$$

The symmetric matrix $F_M F_M^T$ in (4) represents a $(2M+1)$-dimensional orthogonal projection matrix onto the space of signals with small frequencies; therefore, the computation of the truncated series and reconstruction steps taken together form an orthogonal projection of the original sampled function $g(t)$ onto a subspace spanned by the $2M+1$ innermost columns of the rearranged DFT matrix.

Consider a Fourier series expansion of a function $f(t)$ on $t \in [-1, 1]$. Next, select a set of K evenly spaced points $-1 = t_1 < t_2 < \cdots < t_K = 1$ with $t_i - t_{i-1} = 2/(K-1)$. Assume that the Fourier series coefficients F_i, $i = 1, \ldots, K$ for $\mathcal{FS}_K(t)$ have been calculated. Let these values be the elements of a K-vector $\hat{g}$ defined by $\hat{g}_i = F_i$, $i = 1, \ldots, K$. Let M be the number of Gegenbauer polynomials needed for the reconstruction, and let $\alpha > -1/2$ be given. Define G_1 to be a $K \times M$ matrix whose columns are samples of $\widetilde{C}_n^\alpha(t)$. The nth column of G_1 then contains uniformly spaced samples of the Gegenbauer polynomial $\widetilde{C}_n^\alpha(t)$, i.e., $G_1(i, n) = \widetilde{C}_n^\alpha(t_i)$, $i = 1 \ldots, K$, $n = 0, \ldots, M-1$. The approximation of a function $f(t)$ using a set of orthonormal basis functions in the manner described above can be viewed as a least squares approximation of $f(t)$. The least squares approximation of a continuous function y is given by the following theorem [9]:

Theorem 1: Let $\langle \cdot, \cdot \rangle$ be an inner product, and let $\|\cdot\|$ be the norm induced by this inner product, i.e., $\|h\|_2 = \sqrt{\langle h, h \rangle}$. Let $h_1, \ldots, h_M$ be a set of independent functions with respect to this inner product, and let $h_1^*, \ldots, h_M^*$ be an orthonormalization of these functions. Given a function y, the problem of finding the linear combination of $h_1, \ldots, h_M$, i.e., the coefficients $\{\gamma_i\}_{i=1}^M$, which minimizes

$$\left\| y - \sum_{i=1}^{M} \gamma_i h_i \right\|_2. \tag{5}$$

is solved by $\sum_{i=1}^M \langle y, h_i^* \rangle h_i^*$.

To apply Theorem 1 to $\mathcal{FS}_N(t)$ for the ramp function $f(t) = t$, pick $\alpha > 1/2$, and take $h_n^* = \widetilde{C}_n^\alpha$ and $y(t) = \mathcal{FS}_N(t)$, which is the first N terms of the Fourier series expansion for $y(t)$. Here, the inner product $\langle y, h_i^* \rangle$ represents an integral of the product of the function $y(t)$ with the normalized Gegenbauer polynomial $\widetilde{C}_i^\alpha(t)$ and the weight function $(1-t^2)^{\alpha-1/2}$:

$$\langle y, h_i^* \rangle = \left\langle y, \widetilde{C}_i^\alpha \right\rangle = \int_{-1}^{1} y(t)\widetilde{C}_i^\alpha(t)(1-t^2)^{\alpha-1/2}dt.$$

The approximation of the function $y = \mathcal{FS}_N(t)$ using the Gegenbauer polynomials in Theorem 1 is rather remarkable because normally, one tries to minimize the norm of the expression in (5). Here, the approximation obtained is $f(t) = t$ and not $y = \mathcal{FS}_N(t)$, so that the norm of the error function never approaches zero and is approximately equal to $\|\mathcal{FS}_N(t) - t\|_2$. The least squares solution therefore does not give a good approximation to $y = \mathcal{FS}_N(t)$ but approximates $f(t) = t$ instead, which is the desired result.

We now discuss the discrete version of the least squares approximation of the continuous function $g(t)$ by the first M Gegenbauer polynomials. The expansion coefficient c_n represents the inner product $\left\langle g(t), \widetilde{C}_n^\alpha(t) \right\rangle$, i.e.,

$$c_n \equiv \int_{-1}^{1} (1-t^2)^{\alpha-1/2} g(t)\widetilde{C}_n^\alpha(t)dt, \quad n = 0, \ldots, M-1. \tag{6}$$

The coefficients c_n may be calculated with a single matrix-vector product, using the trapezoidal rule [10] for the numerical integration as follows: First, a vector of weights for the trapezoidal rule is defined as the K-vector: $\nu = (2/(K-1))[1/2\ 1\ 1\ \cdots\ 1\ 1\ 1/2]^T$. Define a discrete weight vector $w = [w_1 \cdots w_K]^T$ associated with the Gegenbauer polynomials by $w_i = \left(1-t_i^2\right)^{\alpha-1/2}$, $i = 1, \ldots, K$. Using MATLAB notation, define a $K \times M$ matrix G_2 with column i given

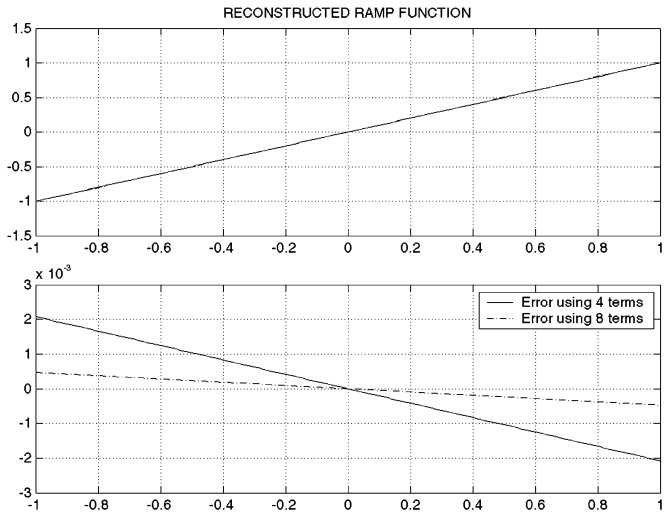

Fig. 3. Reconstruction of ramp function from truncated DFTs.

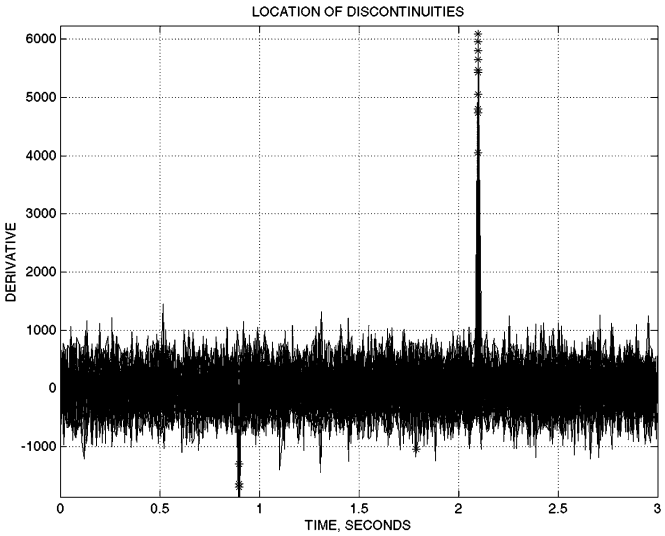

Fig. 4. Location of discontinuities.

by the Hadamard or elementwise product $G_2(:,i) = G_1(:,i).*w.*\nu$, $i = 1,\ldots,M$.

The vector of coefficients $c = [\, c_0 \quad c_1 \quad \cdots \quad c_{M-1}\,]^T$ is then equal to $c = G_2^T\hat{g}$. This product is equivalent to using the trapezoidal rule for integration, which can be viewed as one weight function ν, where $\nu_i = \nu(t_i)$ on the interval $[-1,1]$ with the mesh size equal to $2/(K-1)$ and a second weight function w, $w_i = w(t_i)$ for the Gegenbauer polynomial weight function included. The reconstructed function $\tilde{g}$ can then be calculated as $\tilde{g} = G_1 c = G_1 G_2^T \hat{g}$, which is a weighted sum of the first M orthonormal Gegenbauer polynomials.

V. Denoising of Piecewise Polynomial Signals

In this section, signals $s(t)$, which are piecewise polynomial on an interval $[a,b]$, will be considered. We begin by examining the case where $f(t) \equiv r(t) = t$ on $t \in [-1,1]$. From theory, let auxiliary parameters β and ϵ be defined as $\beta = 2\pi e/27$, and let $\epsilon = (b-a)/2$ [5]. These parameters are then used to define the maximum degree of the Gegenbauer polynomial to be used as the integer M, which is the smallest integer greater than or equal to $\beta\epsilon N$. The parameter α is defined as $\alpha = \beta\epsilon N$. Alternatively, a search for optimal values of M and α is made [4] using the same intervals over which the signal reconstructions are to be made and using functions representative of the functions that are being approximated. Here, this search is performed only once beforehand, and the values for M and α are then held constant for the remaining calculations.

The truncated ramp function $r(t) = t$ on $[-1,1]$ was analyzed using a sample rate of 100 Hz, and the 2 and 4 Hz truncations of the DFT were then reconstructed. The top plot in Fig. 3 gives the ramp function and its two reconstructions, which are indistinguishable in the figure. In the bottom plot of Fig. 3, the differences between the ramp function and each of the two reconstructions are plotted. The values for $M = 3$ and $\alpha = 1.993$ were used. Recalling that $C_1^{\alpha}(t) = 2\alpha t$, the correct solution is $C_1^{1/2}(t) = 2(1/2)t = t$. This is an example of a function that is continuous on an interval except that its first and last values in the interval differ, so that its periodic extension to the entire real axis represents a discontinuous periodic function.

Signals of the form $\exp(s(t))$ arise in a number of applications and the instance where $\log(s(t))$ is a single polynomial is considered in [11]. Here, a piecewise polynomial signal $s(t)$ is considered for $t \in [3]$. The noise is zero-mean additive white Gaussian noise at an SNR of -15 dB. Fig. 5(a) gives the original piecewise continuous signal. Fig. 5(b) gives the sum of the signal and noise. In order to denoise the signal, it is sampled at a rate of 170 Hz, and its DFT is calculated on each continuous segment of the function. Each DFT is truncated to 7 Hz. The locations of the discontinuities were estimated by calculating the derivative of the signal plus noise, as shown in Fig. 4. Fig. 5(c) shows the reconstructions from the three truncated DFTs. It can be seen from this plot that the truncation of the DFT series performs the denoising but with Gibbs oscillations present. In Fig. 5(d), the reconstruction of the original function using the numerical method developed above is given. The mean squared error between the reconstructed signal in Fig. 5(d) and the original function in Fig. 5(a) is 0.192.

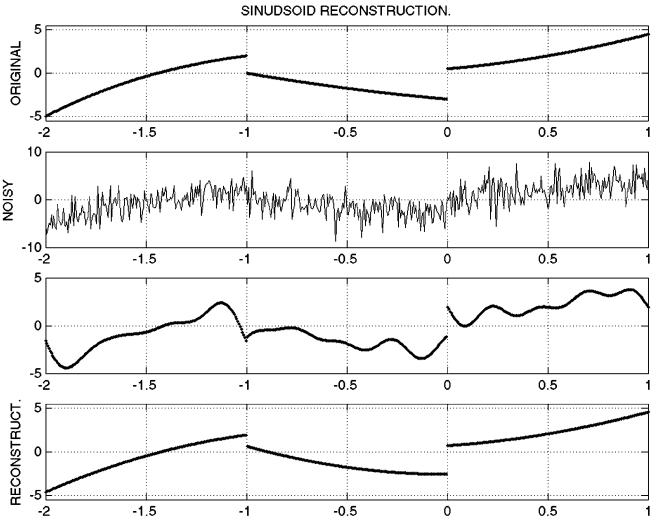

Fig. 5. Denoising using the DFT.

VI. Conclusions

This correspondence discussed the application of recent theoretical results that allow for the accurate reconstruction of a discontinuous

function from a truncated series expansion that contains Gibbs oscillations. It has been demonstrated that when the signal reconstruction is performed using Gegenbauer polynomials, it is possible to remove the Gibbs oscillations from the reconstructed signal. A numerical method was developed and applied to the denoising of a piecewise polynomial signal with multiple discontinuities, and it has been shown that an accurate reconstruction of the original signal can be made from a signal contaminated with Gaussian noise.

REFERENCES

[1] A. Gray and M. Pinsky, "Gibbs phenomenon for Fourier-Bessel series," *Exposition Mathematica*, vol. 11, pp. 123–135, 1993.

[2] S. Durand and J. Froment, "Artifact free signal denoising with wavelets," in *Proc. ICASSP*, Salt Lake City, UT, May 2001.

[3] H. Weyl, "Die gibbssche erscheinung in der theorie der kugelfunktionen," *Gesammeete Abhandlungen*, pp. 305–320, Dec. 1968.

[4] D. Gottlieb and C.-W. Shu, "On the Gibbs phenomenon IV: Recovering exponential accuracy in a subinterval from a Gegenbauer partial sum of a piecewise analytic function," *Math. Comput.*, vol. 64, no. 211, pp. 1081–1095, Jul. 1995.

[5] ——, "On the Gibbs phenomenon and its resolution," *SIAM Rev.*, vol. 39, no. 4, pp. 644–668, Dec. 1997.

[6] H. Dym and H. McKean, *Fourier Series and Integrals*. New York: Academic, 1972.

[7] G. Sansone, *Orthogonal Functions*. New York: Dover, 1991.

[8] M. Abramowitz and I. Stegun, *Handbook of Mathematical Functions*. New York: Dover, 1972.

[9] P. Davis, *Interpolation and Approximation*. New York: Dover, 1975.

[10] E. Isaacson and H. Keller, *Analysis of Numerical Methods*. New York: Wiley, 1966.

[11] S. Golden and B. Friedlander, "Maximum likelihood estimation, analysis and applications of exponential polynomial signals," *IEEE Trans. Signal Process.*, vol. 47, no. 6, pp. 1493–1501, Jun. 1999.

Wideband Time-Varying Interference Suppression Using Matched Signal Transforms

Hao Shen, *Student Member, IEEE,* and
Antonia Papandreou-Suppappola, *Senior Member, IEEE*

***Abstract*—We develop an interference suppression scheme for wideband jamming interference in direct sequence spread spectrum communication systems. We consider interference with time-varying spectral components that can be spread both in time and frequency. Our methodology uses the matched signal transform that is highly localized for signals with nonlinear phase along their frequency-modulation (FM) rate. We compare this method with the use of the more computationally intensive quadratic time-frequency representations whose performance is reduced when the interference is multicomponent.**

***Index Terms*—Frequency modulation, interference suppression, matched signal transform, time-varying signal.**

I. INTRODUCTION

Wireless communication systems are often faced with the problem of jamming interference that could severely distort transmitted information. This interference could be intentional, such as jamming in military communication systems, or unintentional, such as interference from electromagnetic energy emitters. Depending on the application, the interference may be narrowband or wideband; it may also be nonlinear and time-varying (TV) if its spectral components are continuously changing with time in a nonlinear fashion.

Direct sequence spread spectrum (DSSS) techniques have been widely used in personal mobile and military communications [1]. In such systems, narrowband information is spread using a pseudo-noise (PN) sequence before transmission over wireless channels. As the transmission signal is now wideband due to the spreading, it is less susceptible to being distorted when intentionally jammed with a narrowband interference signal, for example, in radar or sonar military applications. Thus, one advantage of spreading techniques is their resistance to jamming interference. As a result, when the processing gain of the system can accommodate high jamming-to-signal ratios (JSRs), no interference cancellation method is required. However, for larger JSR values, efficient suppression techniques must be investigated.

Signal processing techniques aim to suppress interference from received data by transforming it to a different domain, where the characteristics of the interference are more distinguished than in the time domain. Although it is an adequate tool for narrowband jamming interference [2], the Fourier transform (FT) fails to suppress wideband TV interference as the wideband interference is not localized in the frequency domain. Other methods used for narrowband interference excision include lapped transforms [3] and adaptive subband transforms [4], [5]; these methods perform the excision either in the time domain or in the frequency domain, depending on the domain in which the interference is localized. For example, the adaptive subband transform has been applied to interference that is wideband but time localized.

Time-frequency methods such as the Wigner distribution (WD) have been applied to suppress TV interference such as linear frequency-

Manuscript received June 19, 2003; revised July 26, 2004. This work was supported by the National Science Foundation CAREER Award CCR-0134002. The associate editor coordinating the review of this manuscript and approving it for publication was Prof. Fredrik Gustafsson.

The authors are with the Department of Electrical Engineering, Arizona State University, Tempe, AZ 85287-7206 USA.

Digital Object Identifier 10.1109/TSP.2005.849218